




## Natural history of Usher type 2 with the c.2299delG mutation of *USH2A* in a large cohort

Audrey Meunier, Xavier Zanlonghi, Anne-Françoise Roux, Jean-François Fils, Laure Caspers, Isabelle Migeotte, Marc Abramowicz & Isabelle Meunier

To cite this article: Audrey Meunier, Xavier Zanlonghi, Anne-Françoise Roux, Jean-François Fils, Laure Caspers, Isabelle Migeotte, Marc Abramowicz & Isabelle Meunier (2022) Natural history of Usher type 2 with the c.2299delG mutation of *USH2A* in a large cohort, *Ophthalmic Genetics*, 43:4, 470-475, DOI: [10.1080/13816810.2022.2051191](https://doi.org/10.1080/13816810.2022.2051191)

To link to this article: <https://doi.org/10.1080/13816810.2022.2051191>

 View supplementary material 

 Published online: 28 Mar 2022.

 Submit your article to this journal 

 Article views: 86

 View related articles 

 View Crossmark data 

RESEARCH REPORT



## Natural history of Usher type 2 with the c.2299delG mutation of *USH2A* in a large cohort

Audrey Meunier<sup>a</sup>, Xavier Zanlonghi<sup>b</sup>, Anne-Françoise Roux<sup>c,d</sup>, Jean-François Fils<sup>e</sup>, Laure Caspers<sup>a</sup>, Isabelle Migeotte<sup>f</sup>, Marc Abramowicz<sup>f,g</sup>, and Isabelle Meunier<sup>d,h</sup>

<sup>a</sup>Department of Ophthalmology, University Hospital Saint-Pierre, Université Libre de Bruxelles (ULB), Bruxelles, Belgium; <sup>b</sup>Centre de compétence Maladies rares, Jules Verne Clinic, Nantes, France; <sup>c</sup>Laboratory of Molecular Genetics, University of Montpellier, Montpellier University Hospital, Montpellier, France; <sup>d</sup>Institute for Neurosciences of Montpellier, INSERM, University of Montpellier, Montpellier, France; <sup>e</sup>Ars Statistica, Nivelles, Belgium; <sup>f</sup>Genetic department, IRIBHM, Université Libre de Bruxelles, Bruxelles, Belgium; <sup>g</sup>Department of Genetic Medicine and Development, Faculty of Medicine, University of Geneva, Geneva, Switzerland; <sup>h</sup>National center in rare diseases Maolya, Genetics of Sensory Diseases, University Hospital, Sensgene Care Network, Montpellier, France

### ABSTRACT

**Background:** The c.2299delG mutation is prevalent and accounts for 24.5% *USH2A* pathogenic variants, with promising prospects for customized gene therapy.

**Materials and Methods:** We compared the ocular and auditory phenotypes in a retrospective cohort of 169 Usher type 2 patients, with and without the c.2299delG allele, including visual acuity, slit-lamp examination, optical coherence tomography, kinetic perimetry, and audiometric assessment to define the hearing disability. Statistical methods used were covariate balancing propensity score and adjusted survival curves log-rank test for the analysis of visual acuity.

**Results:** We compare 54 Usher patients (31%) carrying at least one c.2299delG allele to 109 patients without this variant. The mean ages at onset of night blindness (14 years) and onset of peripheral vision deficiency (24 years) were similar in both groups, as was the severity of hearing loss ( $p = 0.731$ ), even in homozygotes ( $p = 0.136$ ). Based on the covariate balancing propensity score, the c.2299delG carrier patients developed cataract and reached a BCVA of 20/63 earlier than patients without this mutation (mean age 36 versus 42 y.o.; and 52.2 versus 55.1 y.o., respectively). Using adjusted survival curves and a log-rank test based on inverse probability weighting, patients with the c.2299delG variant reach blindness (BCVA <20/400) at 42.3 years old instead of 79.8 years for other *USH2A* pathogenic variants.

**Conclusions:** We conclude that c.2299delG is associated with a more severe phenotype of the Usher type 2, in homozygotes and in compound heterozygotes.

### ARTICLE HISTORY

Received August 12, 2021

Revised March 01, 2022

Accepted March 04, 2022

### KEYWORDS

Usher; retinitis pigmentosa; c.2299delG; *USH2A*; propensity score

## Introduction

Usher syndrome is the most frequent genetic cause of combined auditory and visual sensory handicap. It is characterized by a variable phenotype and genetic heterogeneity. The prevalence of Usher syndrome is estimated between 1/30000 and 1/6000 (1). According to the degree of congenital, nonprogressive hearing loss (HL) and vestibular disability, three types of Usher syndrome have been described. Usher type 1 (USH1) affects children, who present bilateral and profound sensorineural hearing loss and vestibular areflexia. Usher type 2 (USH2) is characterized by moderate hearing loss allowing language acquisition, and normal vestibular function.

Visual impairment is due to progressive photoreceptor degeneration leading to retinitis pigmentosa (RP) with night blindness, constriction of the visual field (VF), and visual impairment at end stage. In USH1, RP starts in the first decade and in the second or third decade in patients with USH2 type. USH1 and USH2 are the most frequent. Usher type 3 (USH3) is rare except in the Finnish population. Twelve loci are known, and nine genes have been identified: five genes for USH1, three for USH2, and one for USH3 (2). USH2 is the prevalent type of Usher syndrome and accounts

for more than 50% of cases (3). The *USH2A* gene is involved in 80% of USH2 cases (2,4). The *USH2A* gene (OMIM 276901, 1q41) encompasses 72 exons and codes for two alternatively spliced isoforms of Usherin, a short isoform of 1.546 amino acids, and a long isoform of 5.202 amino acids. Usherin is a transmembrane protein expressed in the human cochlea, brain, eye, and kidney (5). Usherin is expressed within the hair bundles of the cochlea and is localized to the apical inner segment recess that wraps around the connecting cilia in photoreceptor cells of the retina (2). Allelic heterogeneity is high, with more than 100 *USH2A* pathogenic or likely pathogenic variants reported (LOVD Database, accessed on 20 October 2021) (6). Several deep intronic variants leading to insertion of a pseudoexon (40–41) have also been identified in *USH2A* (7). The most frequent pathogenic variant, present in 31% of Usher patients, is the c.2299delG; p. (Glu767fs) variant (4,8,9). This change causes a premature stop codon and leads to a non-functional *ush2a* protein.

The important size of *USH2A* gene limits the conventional AAV-mediated gene therapy approach (10). As Usherin contains multiple repetitive domains, the exon skipping approach

is appealing and a mouse model has been designed to validate whether the deletion of the altered exon could restore the reading frame and the production of functional protein (5). When exon 12 of murine *Ush2a* (homolog to human exon 13) was deleted using CRISPR-Cas9, a shortened functional protein is produced and is correctly localized to the cochlea. Furthermore, it was able to rescue auditory function in *Ush2a* *-/-* knockout mice (11). Moreover, the *ush2a* knockout zebrafish is the first animal model that mimicked the complete USH2A phenotype of both auditory disorder and retinal degeneration (12).

In patients with the c.2299delG mutation in *USH2A*, rod photoreceptors seem to express earlier and more aggressively the disease than cones compared to patients with other mutations (13). There is a lack in the literature description of this phenotype due to the small size of the cohorts.

The objective of this study is to determine the natural course of patients with type 2 Usher syndrome (USH2) due to a biallelic mutation in *USH2A* gene and to compare their phenotypes whether they are heterozygous compounds or homozygous for the c.2999delG variant versus patients without this last variant.

## Materials and methods

A clinical and genetic database of a French center specializing in inherited retinal dystrophies was screened for patients with clinical USH2 and proven biallelic pathogenic variants in *USH2A*. Patients with non-syndromic retinitis pigmentosa, uveitis, or ocular trauma were not included in this study. Informed consent for clinical examination and genetic analysis was obtained and signed by all patients. All methods were carried out in accordance with approved protocols of the Montpellier University Hospital, and in agreement with the Declaration of Helsinki. Color photographs were performed with a Nidek non-mydiatic automated fundus camera (AFC 330, Nidek Inc., Japan) and Topcon non-mydiatic fundus camera TRC-NW8 (Topcon Deutschland Medical GmbH, Germany). Fundus autofluorescence and spectral domain ocular coherence tomography (OCT) imaging were completed with a Combined Heidelberg Retina Angiograph + Spectralis OCT device (Heidelberg Engineering, Dossenheim, Germany). Visual fields were tested with a Goldmann perimeter and for only 27 patients within a visual perimeter (MonPack one, Metrovision, Lille, France).

## Molecular diagnosis

DNA extracted from whole blood was analyzed by next-generation sequencing (NGS). Mutations were confirmed by Sanger sequencing. Segregation was studied when we had parent's DNA as a confirmation of the Cis or Trans position. Informed consent was obtained from all patients in accordance with the Declaration of Helsinki.

## Data collection

To estimate the onset age of the RP, we used the onset age of dark adaptation difficulty. Those data as well as the onset age of feeling of restriction of visual field were

systematically recorded. These data are subjective and come from the feeling of a patient to estimate the age of first discomfort in daily life. Best corrected visual acuity (BCVA) and worst visual acuity (WCVA), slit-lamp examination, appearance of the lens, color imaging, fundus autofluorescence, visual fields (VF), and Heidelberg Spectralis spectral domain Optical Coherence Tomography (OCT) scans were collected at each visit with the patient when possible. Full-field Electroretinogram (ERG)-based ISCEV (International Society for Clinical Electrophysiology of Vision) protocol was systematically performed to confirm rod rod dysfunction. Presence and description of cataract types were done by four ophthalmologists using a topographic classification into clear lens, posterior subcapsular cataract, nuclear cataract, or corticonuclear cataract. No densitometry measures were available in this study. Visual impairment (VI) was scaled following the WHO's classification: moderate for VA from 20/70 to 20/160, severe from 20/200 to 20/400, and legally blindness for VA reaching under <20/200. Inability to drive vision was defined when visual acuity was <20/40.

Macular alterations such as intraretinal cysts, macular hole, and pucker were analyzed on multimodal imaging. Thickness of the macula was collected from MAP of Heidelberg OCT software. Lens appearance at slit-lamp examination was reported at each consultation. The onset age of phacosclerosis was defined by the age when it was first reported. Age of cataract surgery was recorded when known. Visual fields were tested on Goldmann perimetry or on Metrovision Perimetry, and the severity of visual field deterioration was scored, thanks to the Esterman Grid.

Hearing disability was measured by audiometry and classified following the BIAP score (International Board of Audio-Phonology) and the vestibular function investigated by caloric vestibular testing, ocular vestibular evoked myogenic potentials (C-VEMPs), and video impulse test (v-HIT).

## Statistical analysis

For demographics and baseline characteristic variables, continuous data were compared by means of T-test when homogeneity of variances, tested with the Bartlett's test, and normality of the residuals, tested with the Shapiro-Wilks test, were reached and means and standard deviations (means  $\pm$  StDev) are reported. When homogeneity of the variance or normality of the residuals was not proved, Wilcoxon signed rank test was performed on ranked data and medians and interquartile ranges (median [Q<sub>25</sub>-Q<sub>75</sub>]) are reported. For count data, the Pearson Chi-Squared test was performed to compare proportions. Lastly, the R package CBPS was used for the propensity score, aiming to equal the two groups (no mutation vs one mutation) on a set of predefined covariates (age at detection and gender) estimating an Average Treatment Effect (ATE) using Covariate Balancing Propensity Score, which has been shown to be superior to traditional logistic regression approaches and boosted classification and regression trees (14). After the propensity score, groups were compared using survival analyses that included the treatment

group effect and the weight resulting from the matching (15,16). For time-to-event analyses, application of propensity scores using inverse probability weighting (IPW), rather than matching, stratification, or adjustment, produces effect estimates with minimal bias (17). We used adjusted survival curves and log-rank test based on IPW proposed by Xie and Liu (18) and implemented in the IPW survival package. We used the software R, version 3.6.2 (R Core Team, 2019), to perform the statistical analyses.

## Results

### Cohort characteristics

In this cohort, 169 patients (95 females/74 males) from 138 families were included with a biallelic mutation in *USH2A* gene; among them 47 patients (27.8%) were compound heterozygotes for c.2299delG and another pathogenic variant, and seven patients (4.1%) were homozygotes. Fifty-four patients (31.95%) of our *USH2A* cohort thus carried at least one c.2299delG allele. In compound heterozygotes, 34 different mutations were associated in trans with the c.2299delG mutation, consisting of missense mutations (47%), truncating mutations (20%), and splicing mutations (33%). For the propensity score, 156 patients were eligible for the analysis.

### Auditory and vestibular phenotype

Scaled with the BIAP classification (see biap.org), HL was, respectively, moderate in 81.7% of patients (21.1% BIAP 3.1 and 60.6% BIAP 3.2) and severe in 18.3% (12.7.1% BIAP 4.1 and 5.6% BIAP 4.2) instead of, respectively, 77.8% of moderate HL and 22.2% of severe HL in patient carrying the c.2299delG. No statistical difference was observed ( $X^2 = 3.2033$ ,  $df = 3$ ,  $p$ -value = 0.3613). Data not scaled with BIAP were not considered.

Severity of HL was not affected by the presence of the c.2299delG mutation ( $p = 0.7313$ ) even in c.2299delG homozygous patients ( $p = 0.136$ ). The mean age at HL diagnosis was not statistically different: 4 y.o. (3–6) and 5 y.o. (3–7) in both groups ( $p = 0.1675$ ) and 6 y.o. (4.3–7.3) for homozygous c.2299delG genotype ( $p = 0.495$ ). Due to the small sample size (only eight patients), statistical analysis on patient with two c.2299delG allele was not significant. As expected, no vestibular areflexia was reported in the cohort (data available for 56/162 patients) (4).

### Ophthalmological phenotype

#### Symptoms and signs of retinitis pigmentosa onset

In this study, 69% of Usher patients carrying the c.2299delG variant reported night blindness at a mean age of 15 y.o. (8–19) and 45% mentioned a feeling of visual field constriction at a mean age of  $25.3 \pm 10.5$  y.o. The age of onset of night blindness is used in this study to estimate the first symptom of RP and did not significantly differ from patients

homozygous or heterozygous compound for c.2299delG variant than those with other *USH2A* genotypes (night blindness  $p = 0.5159$ , clumsiness  $p = 0.9977$ ).

At first consultation, the full-field electroretinogram was performed according to the ISCEV protocol after a dark adaptation of 20 minutes, 100% of patients had no response in scotopic conditions and in photopic conditions, and no response was discernible neither as classically noted in most cases of retinitis pigmentosa regardless of the mutation and gene involved. Only 10% of them showed residual responses at flicker stimulations and the mean amplitude was 19.2 mV. No statistical difference between patients carrying the c.2299delG and other genotypes was possible to observe.

### Visual acuity

At first consultation, 33% of patients with the c.2299delG allele had a visual acuity insufficient for driving (inferior to 20/40), 9% had a BCVA under 20/63 at a mean age of 46 y.o., and 17% were already legally blind due to a visual acuity under 20/400 at a mean age of 52 years. Based on a survival study, 15% of the cohort reached a BCVA under 20/400. The mean age was 42.3 y.o. in patients carrying the c.2299delG variant versus 79.8 y.o. in the rest of the cohort.

**Results after applying the propensity score.** Regarding the visual evolution, the two groups did not show a difference in probability to have a BCVA <20/40 (Survival in the no c.2299delG group: 35.2%; Survival in the c.2299delG group: 22.1%). Patients reached a BCVA <20/40 at a mean age of 47.6 years for the c.2299del group instead of 52.4 years for the other group ( $p = 0.317$ ) (Figure 1a). On the contrary, patients carrying c.2299delG had a higher probability of an earlier BCVA of 20/63 and 20/400 (Survival in the non-c.2299delG group: 86.5%; Survival in the c.2299delG group: 52.1%). Patients reached a BCVA 20/63 at a median age of 52.2 y.o. in the c.2299del group instead of 55.1 y.o. in the other group ( $p = 0.193$ ) (Figure 1b). Patients carrying c.2299delG had a higher probability to become blind (BCVA <20/400) (Survival in the no c.2299delG group: 86.5%; Survival in the c.2299delG group: 52.1%) ( $p = 0.011$ ) (Figure 1c and Fig S1.). Not enough data were available to analyze the c.2299delG homozygous group. (Propensity score was performed after matching patients in age and gender (Table 1).)

### Anterior segment examination

Cataract classically consisted of a posterior capsular opacification leading to a rapid VA degradation. Patients carrying the c.2299delG mutation developed phacosclerosis earlier than the other *USH2A* patients, with a mean age of 36.3 y.o.  $\pm 9.1$  versus 42.2 y.o.  $\pm 12.0$  ( $p = 0.0437$ ) for other genotypes. At the first consultation, 46.8% of patients already presented phacosclerosis, and 9.3% had undergone phacosurgery. No statistical difference between these two subgroups was found regarding the age of phacosurgery: the mean age for the c.2299delG group was  $42.5 \pm 7.8$  versus  $48.6 \pm 12.1$  for other *USH2A* patients ( $p = 0.173$ ).

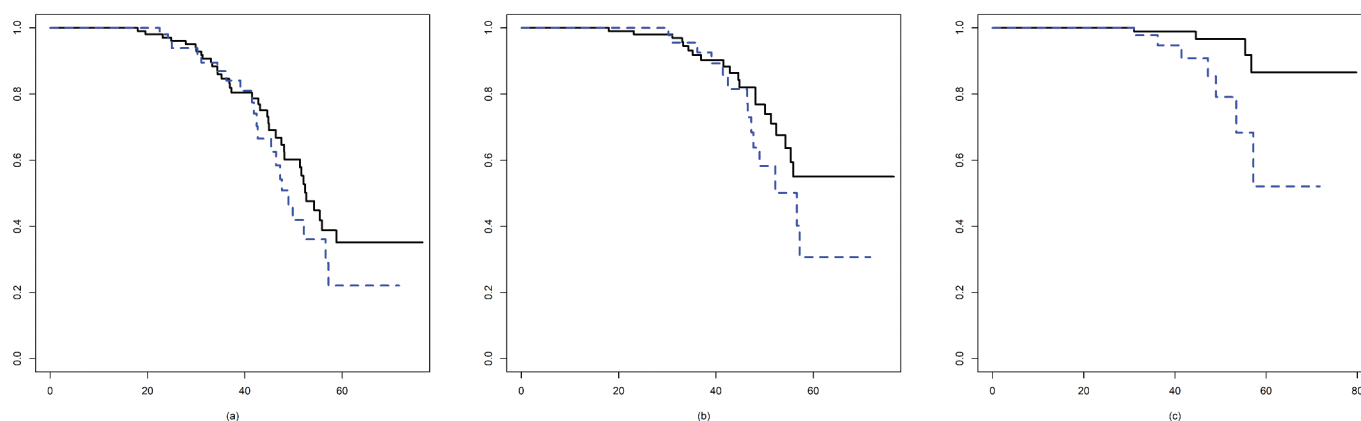


**Figure 1.** Kaplan–Meier-adjusted probability for reaching mild and severe visual impairment and blindness, censored at 60 y.o. Full line curve, c.2299delG absent; dashed curve, c.2299delG present. X axis, age. (a) Y axis, adjusted probability for reaching a BCVA <20/40 (mild impairment). (b) Y axis, adjusted probability for reaching a BCVA <20/63 and ≥20/400 (severe visual impairment). (c) Y axis, adjusted probability for reaching a BCVA <20/400 (blindness).

**Table 1.** Propensity scores.

	Before Matching			After Matching		
	Absence of c.2299delG (n = 109)	Presence of c.2299delG (n = 47)	ASD	Absence of c.2299delG (n = 109)	Presence of c.2299delG (n = 47)	ASD
Age at detection	37.5 (13.56)	36.05 (14.64)	10.30%	37.11 (13.42)	37.11 (14.82)	0.00%
Gender (W)	52.29%	51.06%	2.46%	51.79%	51.79%	0.00%

ASD: Absolute Standardized Difference

The next table presents the results of the propensity score. The first part of the table (Before Matching) reports the means and standard deviations for continuous data and proportions for discrete data in the two groups (Absence of c.2299delG, Presence of c.2299delG), as well as standardized difference, and indicates that in almost all cases, the two groups have different means/proportions for the different variables before matching.

The second part of the table presents the results after matching. We directly observe that mean and standard deviations as well as proportions are now closer between the two studied groups. The standardized difference values indicate that the two groups have now similar means/proportions for the different variables after matching; that is, the absolute standardized difference are equal to 0. Based on this matching table, we consider the both groups with and without c.2299delG Mutation similar on covariates chosen for the propensity score. We then performed a series of survival analyses on the outcomes.

### OCT findings

Intraretinal Cysts prevalence was studied through SD-OCT among 56 *USH2A* patients consulting for the first time (18 bearing the c.2299delG (32.1%) and 38 without the c.2299delG allele (67.9%)). In that c.2299delG group, only five patients had intraretinal cysts (27.8%) versus 14 patients (36.8%) with other *USH2A* genotypes. These frequencies were not significantly different. The mean age of patients presenting these macular cysts at the first consultation was 35.4 y.o. if they carried the c.2299delG mutation and 39.6 y.o. for other *USH2A* genotypes. Data for lamellar hole, macular hole, and ERMs were not significantly different between both groups and were not higher than the frequency in the general population (11).

At first OCT acquisition, the mean age of patients was, respectively, 38 y.o. and 37 y.o. for patients with and without the c.2299delG allele. Based on Heidelberg macular map thickness, no significant difference regarding the c.2299delG presence was reported on the retinal thickness of nasal 1500, nasal 3000, and temporal 1500 and 3000  $\mu\text{m}$  from fovea quadrants (Table 2). Correlation between macular thickness, age, and visual acuity was not statistically significant due to the small size of the samples. No difference was observed regarding the foveolar thickness at first consultation either (Figure 2). Only 20/51 patients had a Heidelberg OCT acquisition, leading to an insuf-

**Table 2.** T-test comparisons.

Cadran	no c.2299delG variant	c.2299delG	p-value
Nasal 1500	282.17 $\pm$ 50.28	298.11 $\pm$ 33.28	0.4206
Nasal 3000	267.91 $\pm$ 41.33	268.00 $\pm$ 33.23	0.9962
Temporal 1500	263.00 $\pm$ 56.33	268.89 $\pm$ 27.75	0.777
Temporal 3000	222.18 $\pm$ 40.83	218.88 $\pm$ 21.84	0.8381

Continuous data were compared by means of T-test when homogeneity of variances, tested with the Bartlett's test, and normality of the residuals, tested with the Shapiro–Wilks test, were reached and means and standard deviations (means  $\pm$  StDev) are reported. When homogeneity of the variance or normality of the residuals was not proved, Wilcoxon signed rank test was performed on rank data and medians and interquartile ranges (median [Q25–Q75]) are reported. We used the software R, version 3.6.2 (R Core Team, 2019), to perform the statistical analyses.

ficient amount of statistical data to allow a robust statistical test. Regarding autofluorescence imaging, no analysis was possible due to the nonavailability of this technique for many patients.

### Discussion

To our knowledge, this study represents the largest cohort of c.2299delG mutant *USH2A* patients. The particular interest of this mutation is due to its prevalence and the prospect of a customized gene therapy. Our study confirms the ancestral c.2299delG mutation of *USH2A* as most prevalent, with 30.1% of

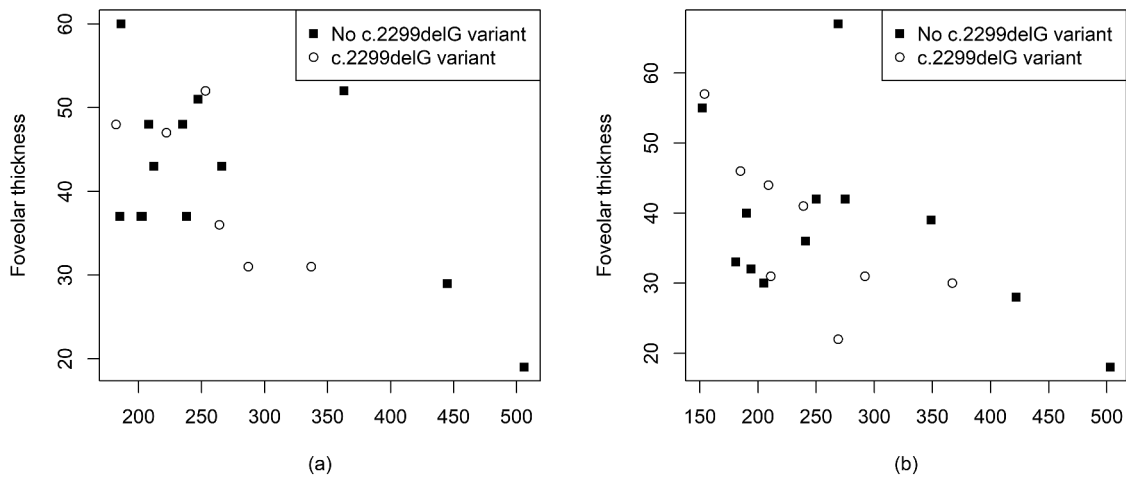


**Figure 2.** This figure represents the foveolar thickness measured by SD OCT Spectralis at first (a) and last (b) contact. White dots represent patient with a c.2299delG allele and black squares other *USH2A* genotype. No difference was observed due to the small size samples.

the *USH2A* patients carrying at least one c.2299delG allele. In the Danish population, the c.2299delG mutation accounts for 45% of all alleles in *USH2* patients (19), 37.7% in UK (8), and 15% in Spain. This gradient from Northern to Southern Europe has been described and is consistent with the hypothesis of a common Scandinavian ancestor (4). Some *USH2A* mutations have been described in Korea as leading to a more severe sensorineural hearing loss (SNHL): c.8176C>T:p(R2723\*), c1823G>A:p.(Cys608Tyr), c.14835delT:p.(Ser4945fs), and c.1312\_13115delAAAT:p.G4371fs but we did not observe those in our cohort (20). Each other mutation was observed in a family only (private mutations). Considering macular complications, intraretinal cysts were present in 28% of patients with the c.2299delG and in 37% of other *USH2A* genotypes. This proportion is smaller than an earlier report of 52% of intraretinal cysts in *USH2A* patients albeit with no distinction of genotypes (19). The present study might be helpful in defining the optimum timing for treating intraretinal cysts before the inner retina becomes too atrophic. Gene therapy or treatment of intraretinal cysts should be proposed before advanced stages of RP. We identified some patients with better macular preservation but could not correlate it with a specific genotype.

Regarding the auditory phenotype, age at HL diagnosis was similar whether the c.2299delG mutation was present or not. As first described by Roux et al., HL in *USH2A* patients is typically mild to severe with a down-sloping configuration. Onset is prelingual, but the diagnosis is usually delayed until 4–6 y.o., with a great variability (ranging from 8 months to 31 y.o.) (21). The median age at Usher syndrome diagnosis was 34.5 y.o., usually after symptoms of RP induced a variable degree of visual disability. In our patients, we observed no mild HL, 81% had moderate HL, and 19% had severe HL. Abadie et al. reported 7% of mild HL, 77% of moderate HL, and 16% of severe HL in *USH2A*. They concluded that in a *USH2* cohort, predicting the mutated gene from audiograms was not possible (21). Penings et al. concluded in 2016 that patients with two truncating mutations developed significantly more severe HL throughout life than others (22). As expected, no vestibular areflexia was reported in this cohort, but data were available only for 56 of 162 patients (18).

This study emphasizes important features of the c.2299delG phenotype.

Firstly, we found a similar decrease of BCVA in both groups until 20/40. However, patients bearing c.2299delG reached the 20/63 (3/10) and 20/400 thresholds earlier than other *USH2A* patients. Considering this difference, c.2299delG patients probably need to be treated earlier than other *USH2A* patients (23). Night blindness was the first reported symptom of RP, and this sign is often used to define the age at RP onset. Data concerning age at onset of night blindness have been collected systematically. However, due to an onset age in childhood and a slow evolution, it often remains uncertain. In addition, the difference between light environment in urban or rural regions differently affects the subjective symptoms of visual disability. The mean age of night blindness onset was 15 y.o. (with a range of 8–20) and was similar in *USH2A* patients with or without the c.2299delG mutation ( $p = 0.5159$ ). Secondly, our study provides evidence to adjust the management and age of phacosurgery in patient with the c.2299delG pathogenic variant. S. Dad et al. reported, in a *USH2A* cohort, a phacosclerosis prevalence of 75% (57/76). The prevalence of c.2299delG was not reported in this study (19). In our *USH2A* cohort, phacosclerosis prevalence at first examination was 54.6% (83/152 patients). This difference may result from the subjective evaluation of phacosclerosis. The use of a densitometer would help to harmonize assessment of the phenotype of lens sclerosis. Our data suggest that phacosclerosis arises sooner in patient bearing c.2299delG than in other *USH2A* patients. Among the c.2299delG group, 46.8% of patients presented unilateral or bilateral phacosclerosis.

## Acknowledgments

The authors would like to acknowledge Professor Christian Hamel for his trust and support. He initiated the study. The authors also thank Professor François Willermain for scientific support, and Catherine Dehon and Judith Racapé for their initial support with statistical methods.

## Disclosure statement

No potential conflict of interest was reported by the author(s).

## Funding

This research received no grants but awards from Foundation Vesale, no grant number known, no APC known, and Foundation Saucez Van-Pouck, no grant number known, no APC known.

## Institutional review board statement

The study was conducted according to the guidelines of the Declaration of Helsinki and approved by the Institutional Review Board of Montpellier University Hospital. The Ministry of Public Health accorded approval for biomedical research under the authorization number 11018S.

## Informed consent statement

Informed consent was obtained from all subjects involved in the study according to the Declaration of Helsinki.

## Data availability statement

The data presented in this study are available on request from the corresponding author. The data are not publicly available due to private medical and genetic information about patients info@drmeunier.be

## References

- Kimberling WJ, Hildebrand MS, Shearer AE, Jensen ML, Halder JA, Trzupek K, Cohn ES, Weleber RG, Stone EM, Smith RJH, et al. Frequency of Usher syndrome in two pediatric populations: implications for genetic screening of deaf and hard of hearing children. *Genet Med*. 2010;12(8):512–16. doi:10.1097/GIM.0b013e3181e5afb8.
- Whatley M, Francis A, Ng ZY, Khoh XE, Atlas MD, Dilley RJ, Wong EYM. Usher syndrome: genetics and molecular links of hearing loss and directions for therapy. *Front Genet*. 2020;11:565216.
- van Wijk E, Pennings RJ, te Brinke H, Claassen A, Yntema HG, Hoefsloot LH, Cremers FPM, Cremers CWRJ, Kremer H. Identification of 51 novel exons of the Usher syndrome type 2A (USH2A) gene that encode multiple conserved functional domains and that are mutated in patients with Usher syndrome type II. *Am J Hum Genet*. 2004;74(4):738–44. doi:10.1086/383096.
- Dreyer B, Brox V, Tranebjærg L, Rosenberg T, Sadeghi AM, Möller C, Nilssen O. Spectrum of USH2A mutations in Scandinavian patients with Usher syndrome type II. *Hum Mutat*. 2008;29(3):451. doi:10.1002/humu.9524.
- Weston MD, Eudy JD, Fujita S, Yao S, Usami S, Cremers C, Greenburg J, Ramesar R, Martini A, Moller C, et al. Genomic structure and identification of novel mutations in usherin, the gene responsible for Usher syndrome type IIa. *Am J Hum Genet*. 2000;66(4):1199–210. doi:10.1086/302855.
- Toualbi L, Toms M, Moosajee M. USH2A-retinopathy: from genetics to therapeutics. *Exp Eye Res*. 2020;201:108330. doi:10.1016/j.exer.2020.108330.
- Slijkerman RW, Vaché C, Dona M, García-García G, Claustres M, Hetterschijt L, Peters TA, Hartel BP, Pennings RJ, Millan JM, et al. Antisense oligonucleotide-based splice correction for USH2A-associated retinal degeneration caused by a frequent deep-intronic mutation. *Mol Ther Nucleic Acids*. 2016;5(10):e381. doi:10.1038/mtna.2016.89.
- Le Quesne Stabej P, Saihan Z, Rangesh N, Steele-Stallard HB, Ambrose J, Coffey A, Emmerson J, Haralambous E, Hughes Y, Steel KP, et al. Comprehensive sequence analysis of nine Usher syndrome genes in the UK National Collaborative Usher Study. *J Med Genet*. 2012;49(1):27–36. doi:10.1136/jmedgenet-2011-100468.
- Vache C, Besnard T, le Berre P, Garcia-Garcia G, Baux D, Larrieu L, Abadie C, Blanchet C, Bolz HJ, Millan J, et al. Usher syndrome type 2 caused by activation of an USH2A pseudoexon: implications for diagnosis and therapy. *Hum Mutat*. 2012;33(1):104–08. doi:10.1002/humu.21634.
- Baux D, Larrieu L, Blanchet C, Hamel C, Ben Salah S, Vielle A, Gilbert-Dussardier B, Holder M, Calvas P, Philip N, Edery P. Molecular and in silico analyses of the full-length isoform of usherin identify new pathogenic alleles in Usher type II patients. *Hum Mutat*. 2007;28(8):781–89. doi:10.1002/humu.20513.
- Pendse ND, Lamas V, Pawlyk BS, Maeder ML, Chen ZY, Pierce EA, Liu Q. In vivo assessment of potential therapeutic approaches for USH2A-associated diseases. *Adv Exp Med Biol*. 2019;1185:91–96.
- Han S, Liu X, Xie S, Gao M, Liu F, Yu S, Sun P, Wang C, Archacki S, Lu Z, et al. Knockout of ush2a gene in zebrafish causes hearing impairment and late onset rod-cone dystrophy. *Hum Genet*. 2018;137(10):779–94. doi:10.1007/s00439-018-1936-6.
- Calzetti G, Levy RA, Cideciyan AV, Garafalo AV, Roman AJ, Sumaroka A, Charng J, Heon E, Jacobson SG. Efficacy outcome measures for clinical trials of USH2A caused by the common c.2299delG mutation. *Am J Ophthalmol*. 2018;193:114–29.
- Imai K, Ratkovic M. Robust estimation of inverse probability weights for marginal structural models. *J Am Stat Assoc*. 2015;110(511):1013–23. doi:10.1080/01621459.2014.956872.
- Austin PC. The performance of different propensity-score methods for estimating differences in proportions (risk differences or absolute risk reductions) in observational studies. *Stat Med*. 2010;29(20):2137–48. doi:10.1002/sim.3854.
- Sekhon JS. Multivariate and propensity score matching software with automated balance optimization: the matching package for R. *Journal of Statistical Software*. 2011;42(7):52.
- Austin PC. The performance of different propensity score methods for estimating marginal hazard ratios. *Stat Med*. 2013;32(16):2837–49. doi:10.1002/sim.5705.
- Xie J, Liu C. Adjusted Kaplan-Meier estimator and log-rank test with inverse probability of treatment weighting for survival data. *Stat Med*. 2005;24(20):3089–110. doi:10.1002/sim.2174.
- Dad S, Rendtorff ND, Tranebjærg L, Grønsvov K, Karstensen HG, Brox V, Nilssen Ø, Roux A-F, Rosenberg T, Jensen H, et al. Usher syndrome in Denmark: mutation spectrum and some clinical observations. *Mol Genet Genomic Med*. 2016;4(5):527–39. doi:10.1002/mgg3.228.
- Lee SY, Joo K, Oh J, Han JH, Park HR, Lee S, Oh D-Y, Woo SJ, Choi BY. Severe or profound sensorineural hearing loss caused by novel USH2A variants in Korea: potential genotype-phenotype correlation. *Clin Exp Otorhinolaryngol*. 2020;13(2):113–22. doi:10.21053/ceo.2019.00990.
- Abadie C, Blanchet C, Baux D, Larrieu L, Besnard T, Ravel P, Biboulet R, Hamel C, Malcolm S, Mondain M, et al. Audiological findings in 100 USH2 patients. *Clin Genet*. 2012;82(5):433–38. doi:10.1111/j.1399-0004.2011.01772.x.
- Hartel BP, Löfgren M, Huygen PL, Guchelaar I, Lo ANKN, Sadeghi AM, van Wijk E, Tranebjærg L, Kremer H, Kimberling WJ, Cremers CW, Möller C, Pennings RJ. A combination of two truncating mutations in USH2A causes more severe and progressive hearing impairment in Usher syndrome type IIa. *Hear Res*. 2016;339:60–68. doi:10.1016/j.heares.2016.06.008.
- Lenassi E, Saihan Z, Bitner-Glindzicz M, Webster AR. The effect of the common c.2299delG mutation in USH2A on RNA splicing. *Exp Eye Res*. 2014;122:9–12. doi:10.1016/j.exer.2014.02.018.